SUPPLEMENTAL MATERIALS FOR:

RAGE binds preamyloid IAPP intermediates and mediates pancreatic β cell proteotoxicity

SUPPLEMENTAL FIGURES AND TABLES

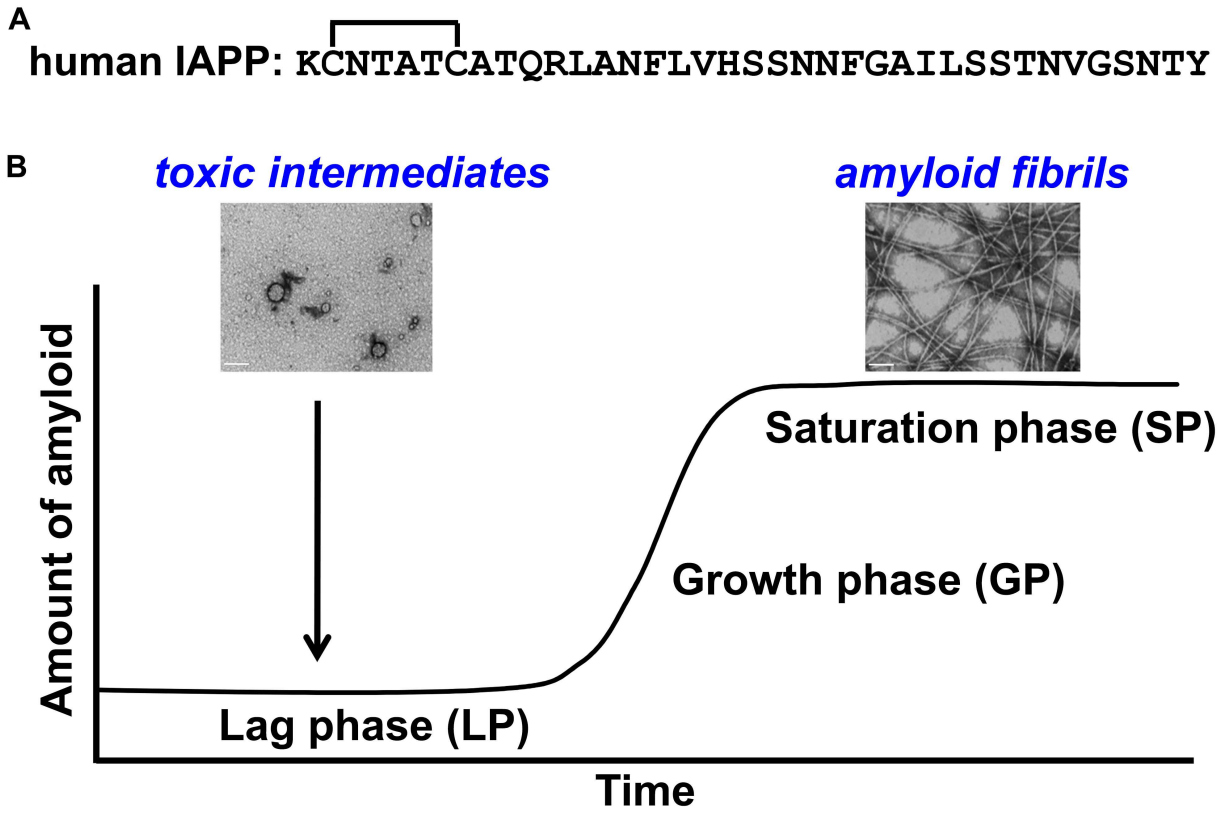

Figure S1. Amyloid formation by h-IAPP. (**A**) Amino acid sequence of wild-type h-IAPP shown using the standard one letter amino acid codes. All IAPP peptides have an amidated C-terminus and a disulfide bridge between residues Cys-2 and Cys-7. (**B**) A schematic diagram representing the kinetics of h-IAPP amyloid formation. Toxic pre-amyloid h-IAPP oligomers form in the lag phase (LP) and assemble into amyloid fibrils in the growth phase (GP). Amyloid fibrils are at equilibrium with soluble protein in the saturation phase (SP).

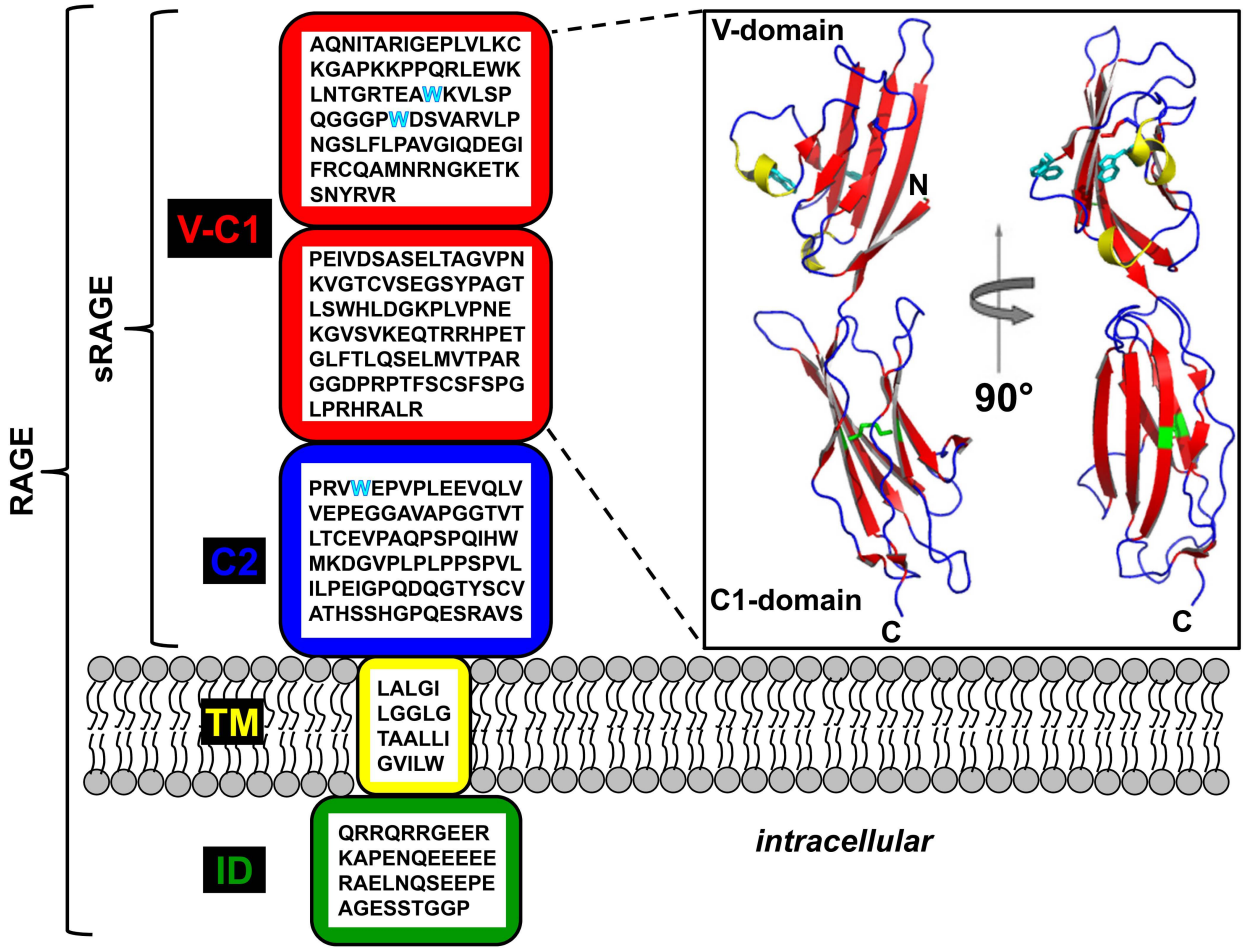

Figure S2. Schematic diagram of the human RAGE protein domains. RAGE is a cell surface protein with three extracellular immunoglobulin-like domains (a V-type domain and two C-type domains), a single transmembrane domain (TM) and a short intracellular domain (ID) that is necessary for signaling. The extracellular V and C1 domains form an integrated structural unit, while C2 is independent, attached to V-C1 through a flexible linker. A basic patch on the extracellular V-C1 domain of human RAGE is believed to be important for binding anionic ligands, while a large hydrophobic patch on the V-domain is postulated to mediate interactions with hydrophobic ligands (1-3). The amino acid composition of each domain is shown by one letter amino acid codes. Solvent exposed Trp residues are indicated in cyan. Far right: A ribbon diagram of the structure of the V-C1 domains: β-sheets (red), β-helices (yellow), loops (blue), disulfide (green), solvent exposed Trp residues (cyan) (PDB code 303U) (2).

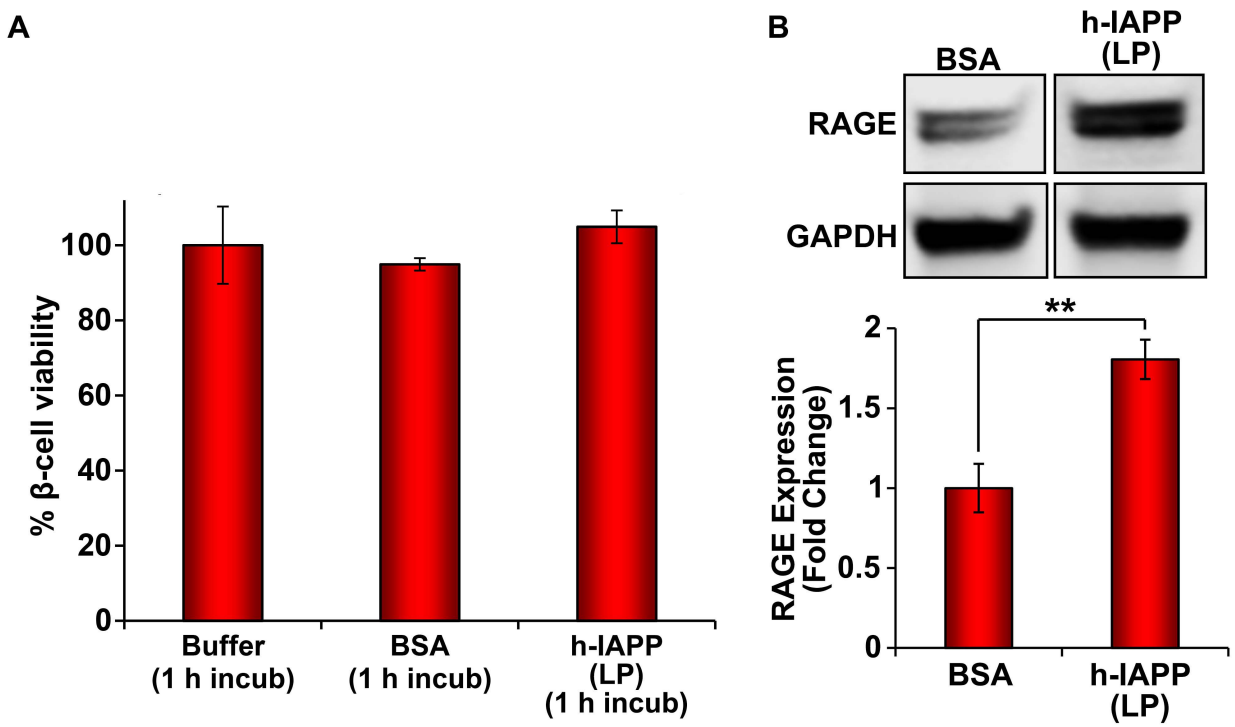

Figure S3. Toxic, pre-amyloid h-IAPP intermediates upregulate RAGE expression in rat INS-1 β-cells prior to inducing cellular toxicity. (**A**) Alamar Blue metabolic assays measuring the viability of β-cells treated (1 h) with h-IAPP LP intermediates or bovine serum albumin (BSA) control. (**B**) Representative WB image of β-cells treated (1 h) with aliquots of the same peptide stock solutions used in β-cell toxicity assays shown in panel **A**. RAGE protein signals are normalized to GAPDH protein signals detected in the same WB lanes. Peptide stock solutions were prepared (20 μM) and incubated (25°C) to produce toxic intermediates. Peptide aliquots were incubated on β-cells for shorter times (1 h) than the standard incubation time (5 h) required to detect measurable loss in metabolic function in our toxicity assays, as shown in Figure 1. Final peptide concentration after transferring peptide aliquots into β-cell assays was 14 μM. WB bands were run on the same gel, but several lanes apart. Data represent mean±SD (toxicity assays) or mean±SEM (WB) of n=3 independent experiments (3-5 technical replicates per experiment). ** $P < 0.01$, two-sample *t*-test.

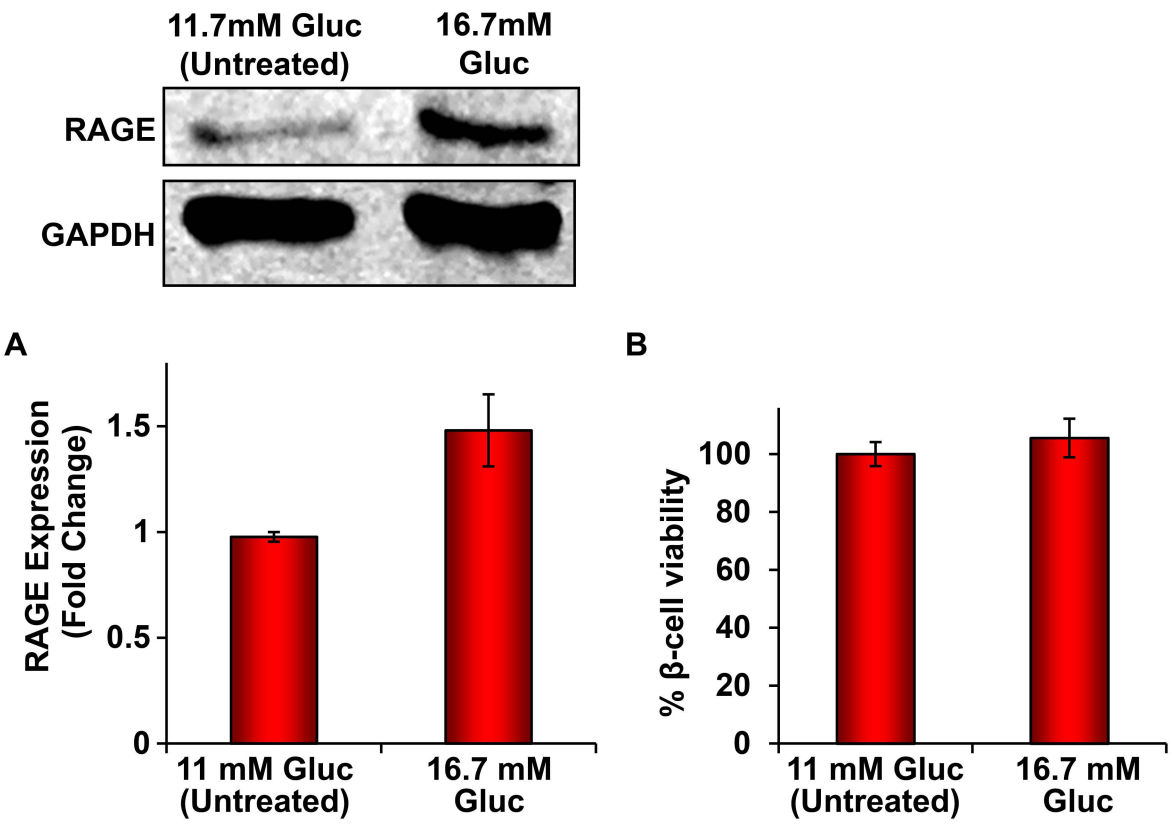

Figure S4. Effect of high glucose incubation on RAGE protein expression in INS-1 β-cells. (**A**) Representative WB images showing a non-significant trend towards increased RAGE protein levels in β-cells incubated (5 h) in high glucose (16.7 mM) compared to standard glucose (11.7 mM) concentrations used to maintain this cell line in culture. RAGE expression is normalized to GAPDH levels. (**B**) Alamar Blue metabolic assays measuring the viability of β-cells incubated (5 h) in high glucose or standard glucose concentrations were simultaneously carried out with WB studies shown in panel **A**. WB bands were run on the same gel contiguously in side-by-side lanes. Data represent mean±SD (toxicity assays) or mean±SEM (WB) of n=3 independent experiments (3-5 technical replicates per experiment), Kruskal-Wallis test.

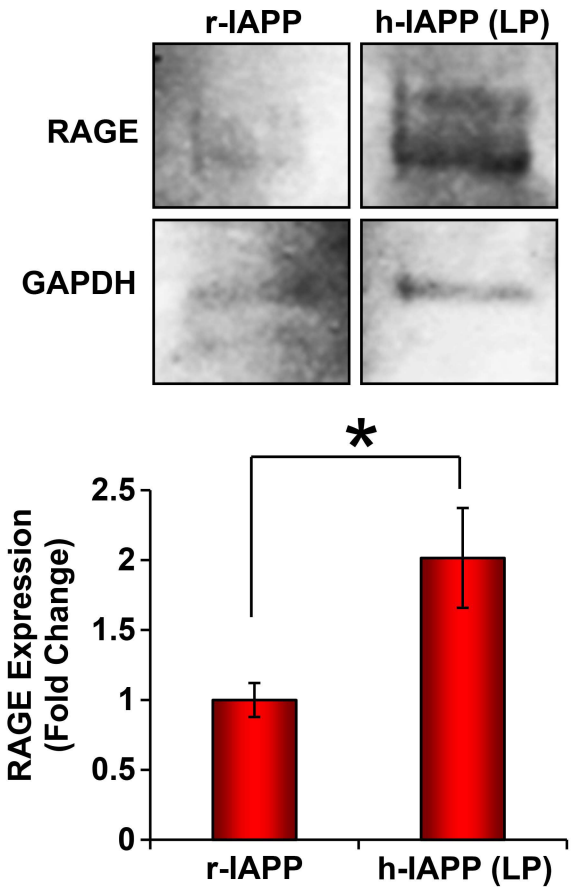

Figure S5. Toxic, pre-fibrillar h-IAPP intermediates upregulate RAGE expression in primary murine pancreatic islets. A representative WB image of lysates obtained from isolated WT murine islets that were incubated (3 h) with either toxic h-IAPP LP intermediates or non-toxic r-IAPP. The WB results show that RAGE protein normalized to GAPDH is upregulated by pre-amyloid h-IAPP intermediates compared to r-IAPP. Peptide stock solutions were prepared (20 μM) and incubated (25°C) to produce aggregates. The toxicity of the peptide solutions were confirmed by Alamar Blue metabolic assays at the same time, shown in Figure 6B. Final peptide concentration after transferring aliquots of peptide into islet assays was 14 μM. WB bands were run on the same gel several lanes apart. Data represent mean±SEM of n=3 replicate experiments. *$P < 0.05$, Kruskal-Wallis test.

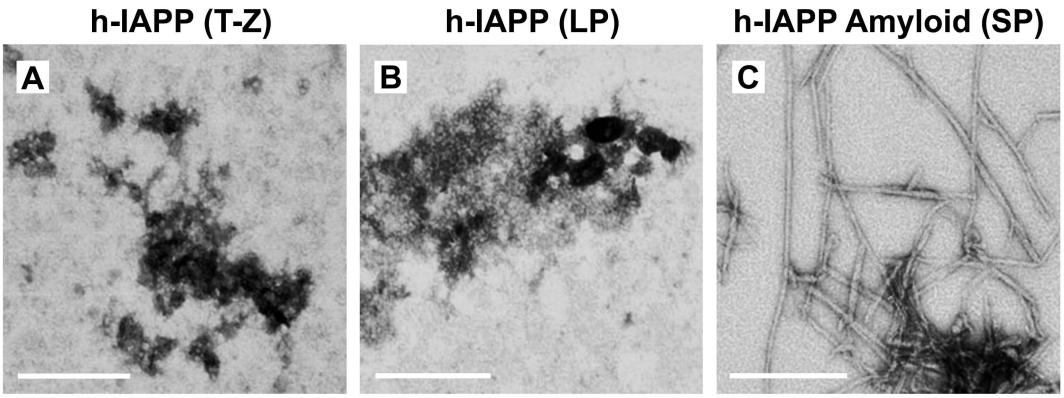

Figure S6. TEM images confirm that RAGE binds only to pre-fibrillar h-IAPP LP species during SPR studies. TEM studies were carried out in parallel with SPR studies shown in Figure 2E to confirm the presence or absence of amyloid fibrils in aliquots of h-IAPP solutions used in SPR experiments: (**A**) amorphous species at time-zero (T-Z), (**B**) toxic pre-fibrillar lag phase (LP) species and (**C**) amyloid fibrils formed in the saturation phase (SP) (scale bars: 200 nm).

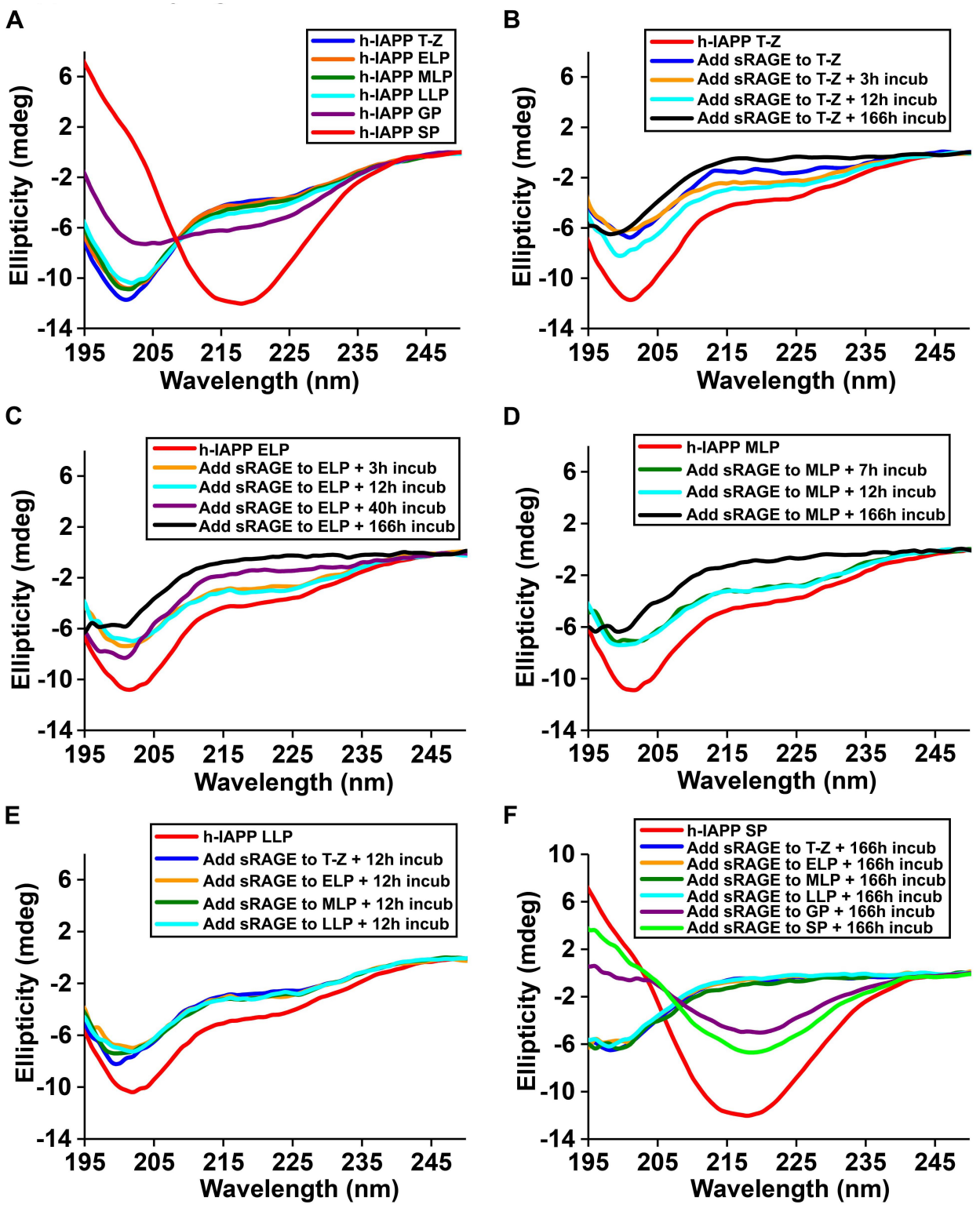

Figure S7. sRAGE inhibits h-IAPP β-sheet formation when added early in the lag phase. (**A**) h-IAPP CD data were collected as a function of time to assess the secondary structure of distinct kinetic species formed over the course of amyloid formation: time-zero species (T-Z, blue), early lag phase (ELP) species (orange), mid-lag phase (MLP) species (dark green), late lag phase (LLP) species (light blue), growth phase (GP) fibrillar species (purple) and saturation phase (SP) amyloid

fibrils (red). (**B-F**) Difference CD of h-IAPP after a 1:1 molar addition of sRAGE to h-IAPP were collected at different time points during the time course of amyloid formation in order to assess the effect of sRAGE on distinct kinetic species: (**B**) sRAGE was added to h-IAPP at T-Z and data collected as a function of time: 0 h after addition of sRAGE to h-IAPP (blue), 3 h after addition of sRAGE to h-IAPP (orange), 12 h after addition of sRAGE to h-IAPP (light blue) and 166 h after addition of sRAGE to h-IAPP (black). Data show a random coil conformation for all conditions, similar to h-IAPP by itself at T-Z (red). (**C**) sRAGE was added to h-IAPP ELP species and data collected as a function of time: 3 h after addition of sRAGE to h-IAPP (orange), 12 h after addition of sRAGE to h-IAPP (light blue), 40 h after addition of sRAGE to h-IAPP (purple) and 166 h after addition of sRAGE to h-IAPP (black). Data show a random coil conformation for all conditions, similar to that of the solution of h-IAPP ELP species by themselves (red). (**D**) sRAGE was added to h-IAPP MLP intermediates and data collected as a function of time: 7 h after addition of sRAGE to h-IAPP (green), 12 h after addition of sRAGE to h-IAPP (light blue) and 166 h after addition of sRAGE to h-IAPP (black). Data show a random coil conformation for all conditions, similar to the solution of h-IAPP MLP species by themselves (red). (**E**) sRAGE was added to h-IAPP T-Z species (blue), ELP species (orange), MLP species (dark green) and LLP species (light blue) and data were collected after an additional 12 h of incubation. The results show comparable random coil conformation to that observed for the solution of h-IAPP LLP species by themselves (red). (**F**) sRAGE was added to h-IAPP T-Z species (blue), ELP intermediates (orange), MLP species (dark green), LLP species (light blue), GP fibrillar species (purple) and SP amyloid fibrils (light green) and data were collected after an additional 166 h of incubation. h-IAPP SP amyloid fibrils by itself (red), incubated for the same amount of time, were used as controls. The results demonstrate that addition of sRAGE to h-IAPP at early time points in the lag phase prevents β-sheet formation; the effect decreases as sRAGE is added at later time points in the lag phase and sRAGE does not prevent β-sheet formation when added after the lag phase. The final peptide concentration was 20 μM in single peptide samples and 40 μM in 1:1 molar mixtures with sRAGE. Assays were carried out in 20 mM tris HCl (pH 7.4, 15°C).

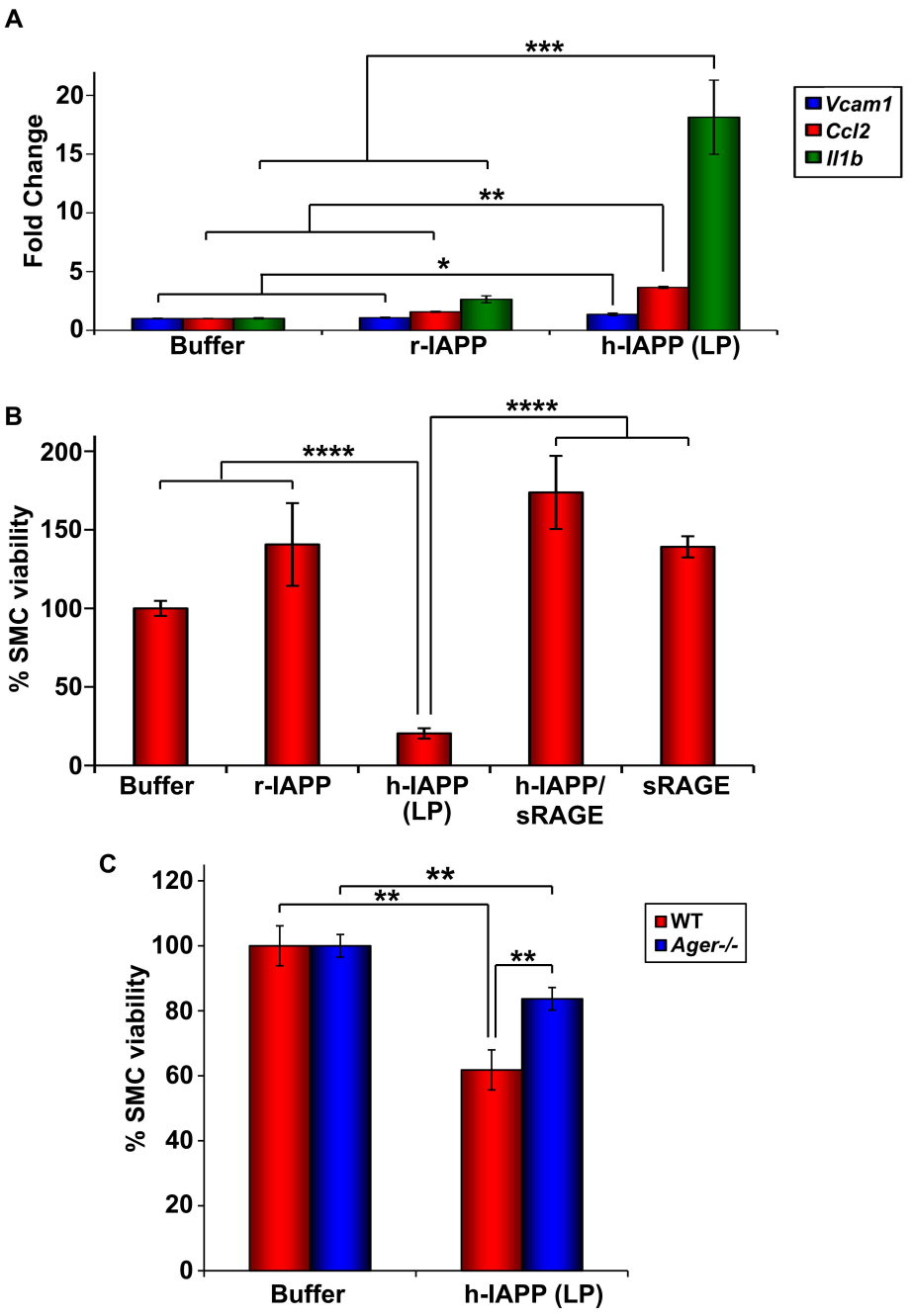

Figure S8. Effect of h-IAPP on primary murine aortic smooth muscle cell (SMC) inflammatory gene expression and toxicity. (**A**) qPCR for the indicated mRNA transcripts of primary murine SMCs incubated with toxic h-IAPP LP intermediates, r-IAPP or buffer solutions. (**B**) Alamar Blue metabolic assays measuring the viability of murine aortic SMCs after treatment with h-IAPP intermediates in the presence or absence of sRAGE or control solutions. (**C**) Alamar Blue metabolic assays show that genetic deletion of *Ager* protects vascular SMCs from h-IAPP toxicity. *Ager*-/- (blue) SMCs show significant resistance to h-IAPP-induced loss in metabolic function relative to WT (*Ager*+/+) SMCs (red). Data represent mean±SD (toxicity assays) or mean±SEM (qPCR studies) of a minimum of n=3 independent experiments (3-6 technical replicates per experiment). *$P < 0.05$, **$P \leq 0.01$, ***$P \leq 0.001$, ****$P \leq 0.0001$; one-way ANOVA or Kruskal-Wallis test, as appropriate.

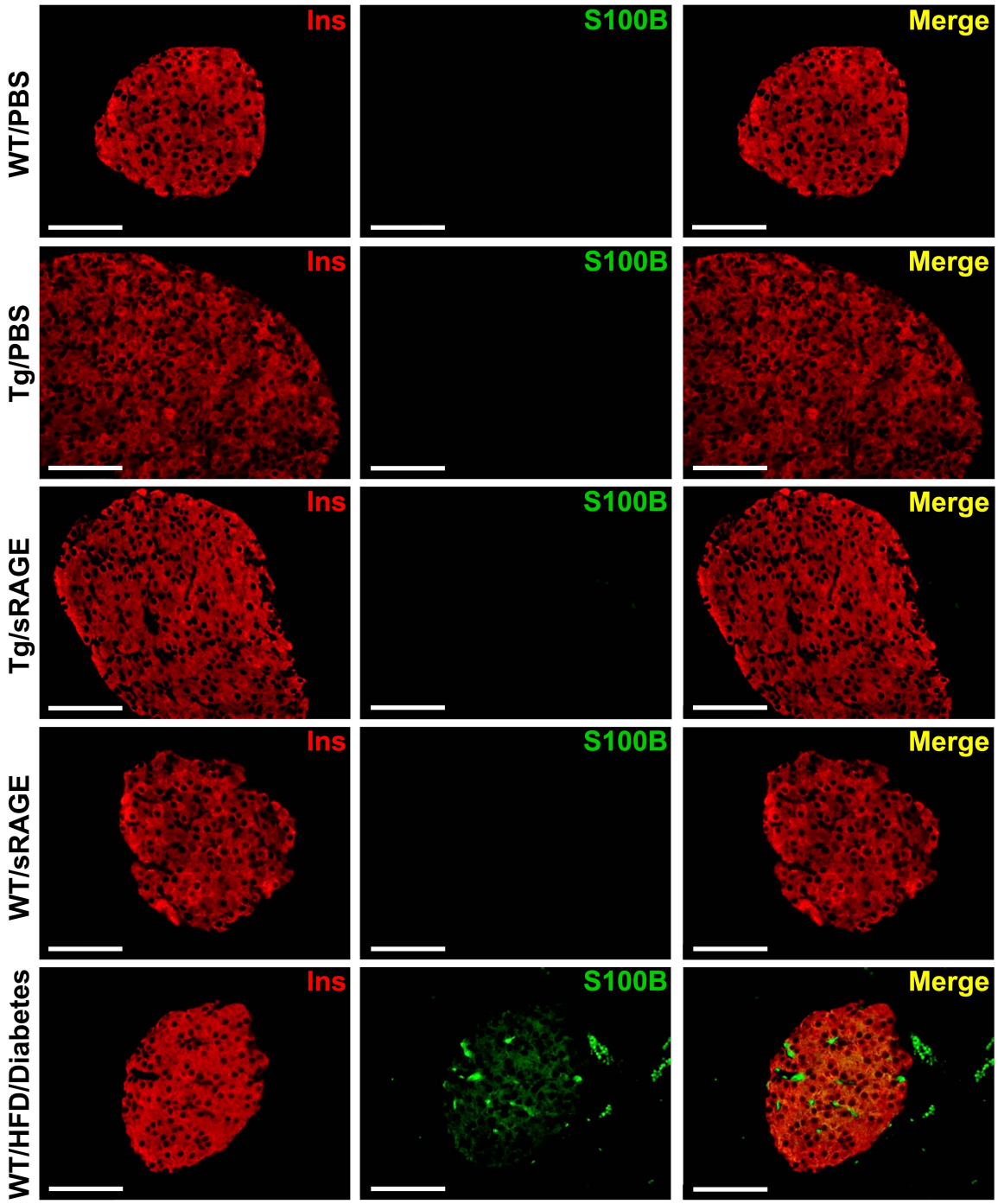

Figure S9. S100b is not upregulated with islet amyloid deposition in hemi_h-IAPP mice. Representative murine islets in pancreas sections co-stained for insulin (Ins, red) and S100b (green) show no significant S100b immunoreactivity in Tg/PBS mice, Tg/sRAGE mice or PBS- or sRAGE-treated WT littermates, consistent with lack of hyperglycemia in these mice. High fat diet-fed (HFD-fed) hyperglycemic (diabetic) WT mice were used as positive controls (scale bar: 75 μm).

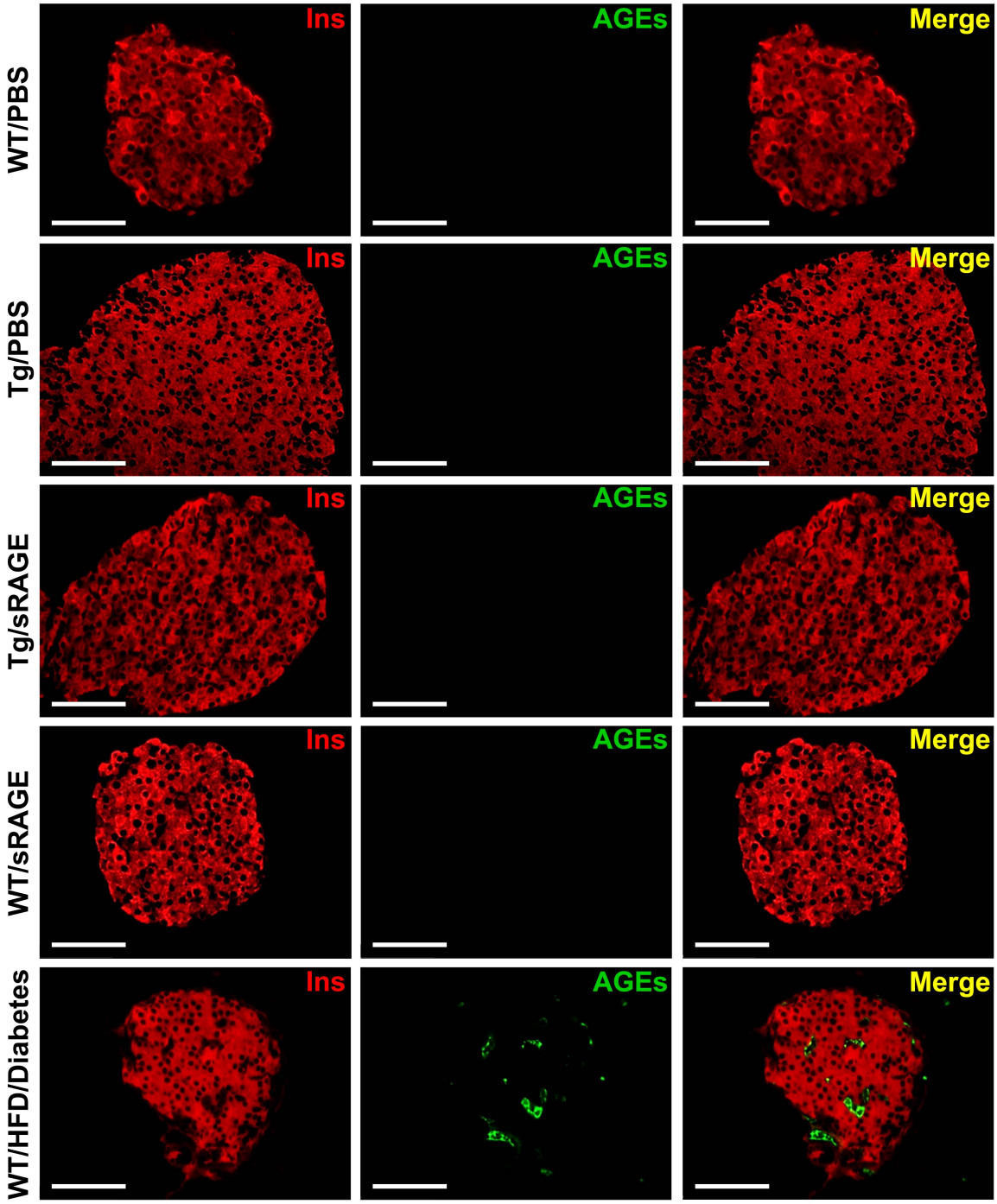

Figure S10. AGEs do not accumulate with islet amyloid deposition in hemi_h-IAPP mice. Representative murine islets in pancreas sections co-stained for insulin (Ins, red) and AGEs (green) show no significant AGE immunoreactivity in Tg/PBS mice, Tg/sRAGE mice or PBS- or sRAGE-treated WT littermates, consistent with lack of hyperglycemia in these mice. HFD-fed hyperglycemic (diabetic) WT mice were used as positive controls (scale bar: 75 μm).

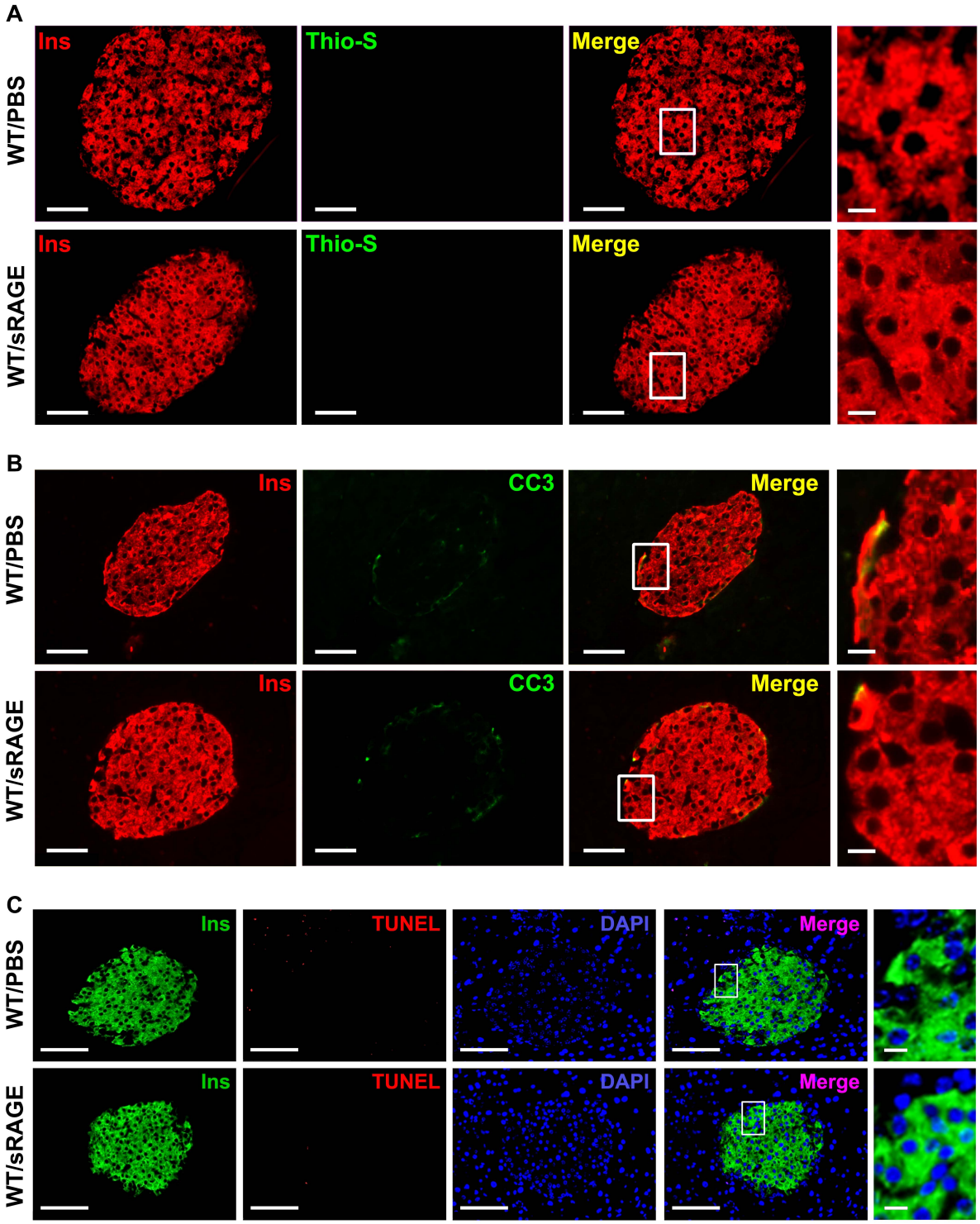

Figure S11. WT control mice display no significant islet amyloid deposition, β-cell stress or apoptosis. Representative immunofluorescence images of the indicated murine islets co-stained in pancreas for (**A**) insulin (Ins, red) and thioflavin-S (Thio-S, green), (**B**) insulin (red) and cleaved caspase-3 (CC3, green) and (**C**) insulin (green), TUNEL (red) and Dapi (blue) (scale bars: 50 μm). White boxes in the merged panels indicate β-cell regions shown at higher magnification in the far right images (scale bars: 8 μm).

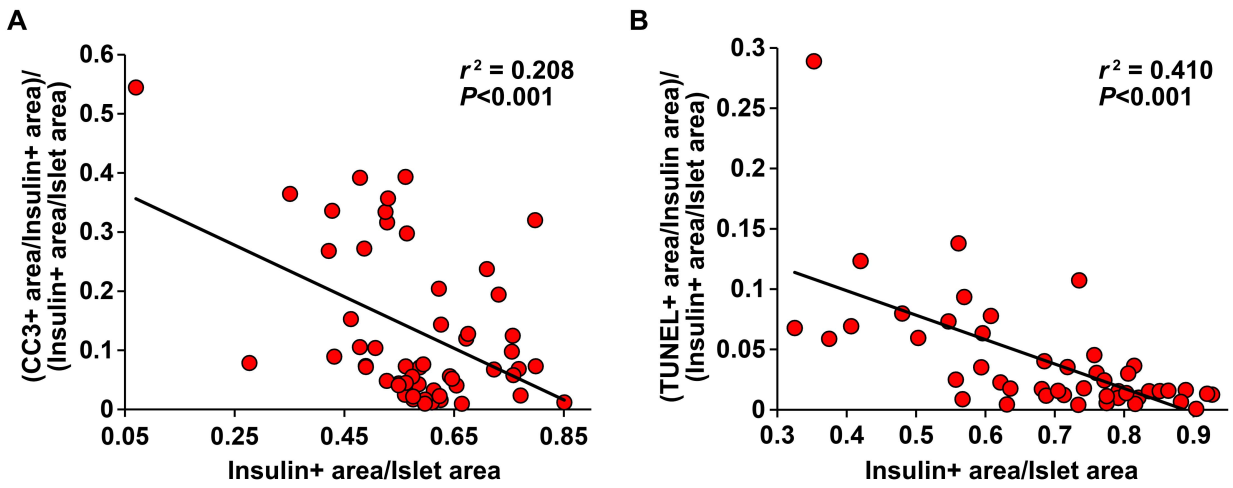

Figure S12. Loss of β-cell area in hemi_h-IAPP mice directly correlates with β-cell stress and apoptosis. Linear regression analysis of histological data from Tg/PBS mice pancreas indicate a negative association between total islet β-cell area and (**A**) β-cell stress/pre-apoptosis ($P < 0.001$, $r^2 = 0.208$) and (**B**) β-cell apoptosis ($P < 0.001$, $r^2 = 0.410$). Data was statistically analyzed by the Wald test.

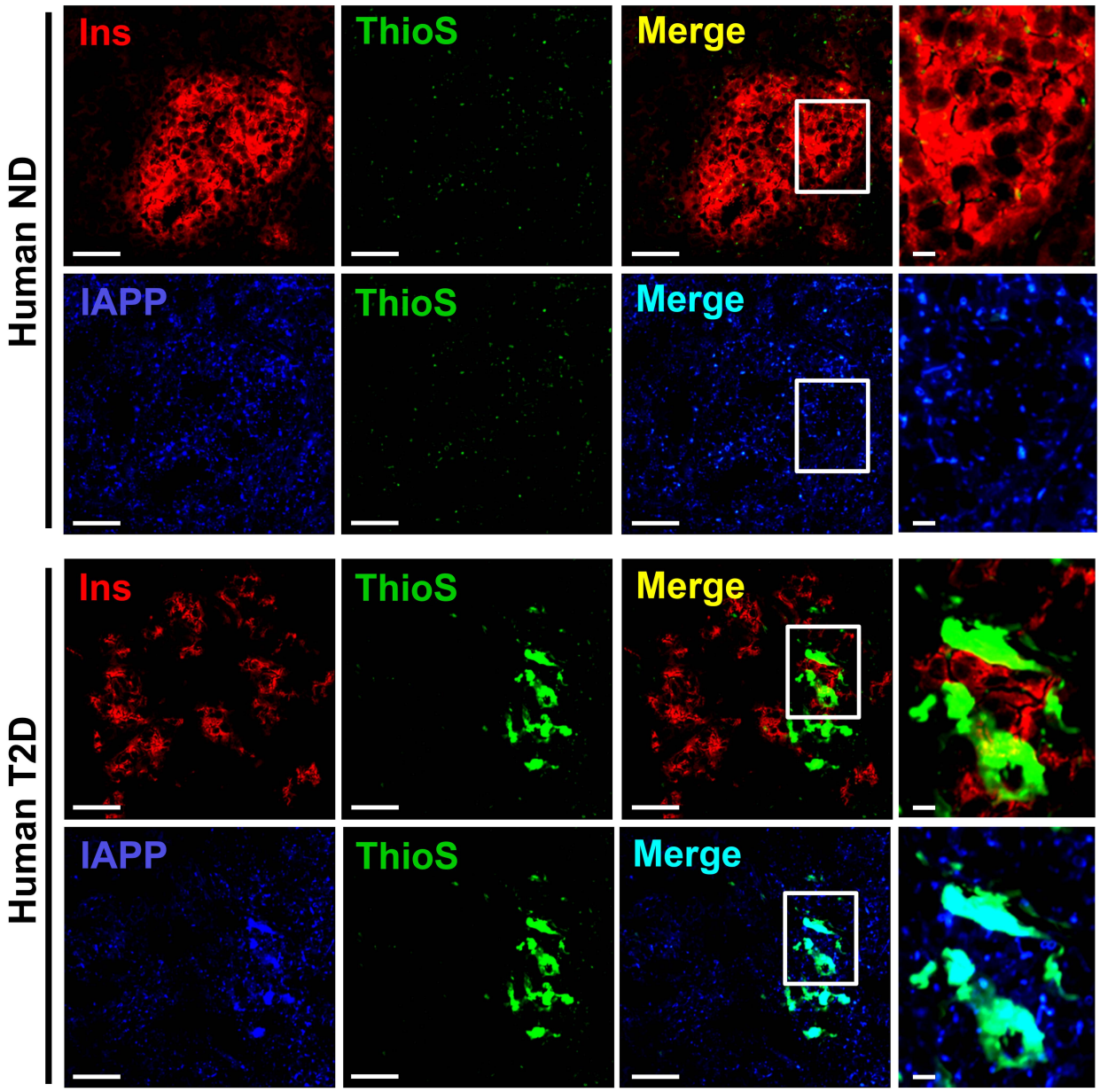

Figure S13. Amyloid plaques derived from h-IAPP spatially overlap with insulin-negative islet areas in human T2D. Representative islets in pancreas from the T2D (nPOD ID 6124) and ND (nPOD ID 6011) human subjects discussed in Figure 11, were also triple-stained for insulin (Ins, red), h-IAPP (blue) and thioflavin-S (Thio-S, green) to confirm the presence or absence of islet amyloidosis. Immunofluorescent images show spatial overlap between insulin(-) (black) and thioflavin-S(+) islet areas, and co-localization (cyan) of thioflavin-S(+) and h-IAPP(+) islet areas in T2D; consistent with h-IAPP derived amyloid and islet amyloidosis-induced loss of β-cell area. Blue h-IAPP(+)/thioflavin-S(-) islet areas suggest that the anti-amylin antibody also detects non-fibrillar forms of h-IAPP (scale bars: 50 μm). No significant amyloid was detected in ND subjects. White boxes indicate islet regions that are shown at higher magnification in the far right images (scale bars: 8 μm).

Analysis (Mean ± SEM)	Calculations	WT/ PBS	WT/ sRAGE	Tg/ PBS	Tg/ sRAGE	Figures and Measurements
% Islet β-cell area	(Insulin+ area / Islet area) x 100	72.4 ± 3.6	73.6 ± 2.9	59.3 ± 2.7	72.2 ± 2.0	Figure 9C (mean of the mean of Thio-S, CC3, TUNEL & RAGE co-stained islets)
% Islet amyloid severity	(Thio-S+ area / Islet area) x 100	N/A	N/A	2.7 ± 0.7	0.3 ± 0.1	Figure 9B (mean of Thio-S/insulin co-stained islets)
% CC3+ β-cell area	(CC3+ area / Insulin+ area) x 100	0.5 ± 0.2	0.5 ± 0.02	6.9 ± 1.1	2.6 ± 0.4	Figure 9E (mean of CC3/insulin co-stained islets)
% TUNEL+ β-cell area	(TUNEL+ area / Insulin+ area) x 100	0.2 ± 0.08	0.2 ± 0.08	2.4 ± 0.7	0.5 ± 0.2	Figure 9G (mean of TUNEL/insulin/DAPI triple-stained islets)
% RAGE+ β-cell area	(RAGE+ area / Insulin+ area) x 100	2.8 ± 0.5	N/A	6.2 ± 0.6	N/A	Figure 10B (mean of RAGE/insulin co-stained islets)
% β-cell stress or pre-apoptotic β-cells	(% CC3+ β-cell area) x (% Islet β-cell area) / 100	~0.36	~0.37	~4.1	~1.9	Calculated using Figure 9C and 9E
% Apoptotic β-cells	(% TUNEL+ β-cell area) x (% Islet β-cell area) / 100	~0.15	~0.15	~1.4	~0.36	Calculated using Figure 9C and 9G
% β-cell RAGE expression	(% RAGE+ β-cell area) x (% Islet β-cell area) / 100	~2.03	N/A	~3.7	N/A	Calculated using Figure 9C and 10B

Table S1. Quantitative immunohistochemical studies of murine pancreas samples. Formalin-fixed paraffin-embedded pancreas sections from PBS- and sRAGE-treated Tg and WT mice (n=3 per grp) were stained and immunofluorescence images were analyzed by morphometry analysis, as described in the Methods and Supplemental Methods sections. Data (mean±SEM) and calculation methods for quantitative analysis of mean % islet β-cell area, % amyloid severity, % β-cell stress and apoptosis, and % β-cell RAGE expression are presented.

nPOD ID	Disease State	Age (y)	Gender	BMI	Diabetes Duration (y)	# of Islets Analyzed	% β-cell RAGE expression (RAGE area / Insulin area)
6009	ND	45	M	30.6		28	24.7 ± 1.1
6011	ND	46	F	26.3		30	52.4 ± 2.3
6021	ND	72	F	24.5		36	23.3 ± 0.9
6102	ND	45.1	F	35.1		34	44.4 ± 1.4
6290	ND	58	M	22.5		33	52.3 ± 2.2
6295	ND	47	F	30.4		30	31.4 ± 1.9
6336	ND	14.3	F	28.9		28	53.4 ± 2.1
6124	T2D	62.3	M	33.7	3	25	52.5 ± 5.6
6133	T2D	45.8	F	40.2	20	23	29.5 ± 3.0
6157	T2D	74.2	F	39.5	1	26	79.1 ± 2.9
6259	T2D	57	M	32.3	10	27	82.1 ± 2.6
6277	T2D	48	M	29.5	10	30	81.1 ± 4.9
6304	T2D	52	F	37.9	25	34	80.2 ± 3.5
6308	T2D	13	F	34.1	1	33	67.5 ± 2.3
6329	T2D	49	F	36.4	25	32	56.6 ± 5.5

Table S2. Clinical and immunohistochemical data for individual human subjects studied. Formalin-fixed paraffin-embedded pancreas sections from de-identified human T2D (n=8) and ND (n=7) subjects were obtained from the Network for Pancreatic Organ Donors with Diabetes (nPOD). The nPOD-designated donor ID's, donor disease states, age, gender (male, M; female, F) and diabetes duration are reported for each subject. Quantitative immunofluorescence image analysis data for mean percent RAGE(+) islet β-cell area is presented for each subject. Data represent mean±SEM. The mean percentages of RAGE(+) islet β-cell area in T2D and ND subjects is presented in main Figure 11B.

SUPPLEMENTAL METHODS

Mice studies. Hemizygous Tg mice (FVB background) that overexpress the amyloidogenic h-IAPP coding sequence under the regulation of the rat insulin II promoter/5' UTR (Jackson Laboratories) (4, 5), were cross bred with WT mice (FVB background) to produce hemizygous Tg h-IAPP (hemi_h-IAPP) mice or WT littermates. Male mice were maintained on a normal chow diet and treated with 100 μL intraperitoneal (i.p.) injections of either sRAGE (100 μg/mL) or vehicle (PBS) 6 days a week for 10 months (starting from 2 months until 12 months of age) to produce 4 age-matched study groups: Tg/PBS, Tg/sRAGE, WT/PBS and WT/sRAGE. Body weight, fasting blood glucose and ipGTT (via injection of 2 g glucose per kg body weight) were measured over the course of the study. Fasting plasma insulin measurements and analysis of islet size, morphology and pathology by histological methods were carried out after sacrifice. Mice were fasted for 5 h before sacrifice and collection of pancreas, spleen (control tissue) and blood for analysis. Fasting blood glucose was measured using a glucometer and fasting plasma insulin was measured using an ultrasensitive insulin ELISA kit (Alpco).

Immunofluorescence (IHC-IF). All murine and human pancreas sections (Formalin-fixed, paraffin-embedded, 4 μm thick) were stained with insulin antibody (1:400, Dako, A0564) to visualize β-cells, and co-stained with either 5% thioflavin-S (Sigma Aldrich, T1892-25G) to detect amyloid deposits; cleaved caspase-3 (Asp 175) antibody (1:100, Cell Signaling, 9661) to detect stress/pre-apoptotic cells; TUNEL (TMR red In Situ Cell Death Detection Kit, Roche, 12156792910) to detect apoptotic cells; RAGE antibody (1:75, GeneTex, GTX27764); AGE antibody (1:200, Abcam, ab23722) or S100B antibody (1:100, Abcam, ab52642) to assess RAGE ligands; or amylin R10/99 antibody (1:60, AbD Serotec, MCA1126) to detect h-IAPP. Staining was carried out by blocking pancreatic sections in PBS containing 2.0% normal goat serum (Vector Laboratories) and incubating with primary antibody diluted in PBS/1% BSA, followed by incubation with secondary antibody diluted in PBS for 1 h. Secondary antibodies for immunolabeling of insulin (1:100, Alexa Fluor 594-conjugated (A11076) or Alexa Fluor 488-conjugated (A11073) goat anti-guinea pig immunoglobulins), cleaved caspase-3 (1:100, Alexa Fluor 488-conjugated goat anti-rabbit immunoglobulins, A11304), RAGE (1:100, Alexa Fluor 488-conjugated donkey anti-goat immunoglobulins, A11055), AGE (1:100, Alexa Fluor 488-conjugated goat anti-rabbit immunoglobulins, A11304), S100B (1:100, Alexa Fluor 488-conjugated goat anti-rabbit immunoglobulins, A11304), h-IAPP (1:100, Cascade Blue-conjugated goat anti-mouse immunoglobulins, C962) were all purchased from Invitrogen. Sections were counterstained with Dapi anti-fade mounting media (2 μg/mL; Invitrogen) to identify nuclei. Immunofluorescence images were taken using a Leica fluorescent microscope, and quantitative analysis was carried out using MetaMorph LASF imaging software.

Histological measurements were carried out as indicated in Table S1. Morphometry immunofluorescence image analysis for amyloid, insulin, CC3, TUNEL, RAGE and islet size (reported as mean islet diameter ±SD) was carried out by first calculating the mean islet data for each mouse (n=15-49 islets per mouse); and then calculating the mean of the mean islet data for each group (n=3 mice per group). IHC analysis for RAGE immunoreactivity is not shown for Tg/sRAGE and WT/sRAGE mice because i.p. administration of sRAGE yields false-positive data in these groups, as the RAGE epitope recognized by the anti-RAGE antibody is also present in sRAGE. All measurements, except for those shown in linear regression plots, are expressed as percentages. The data in linear regression analyses presented in Figures 10C, S12A and S12B are derived from Tg/PBS mice and are shown as the absolute values of fractions normalized to total β-cell area, similar to previous reports (6). The formulas used to calculate all measurements are

presented in Table S1, and also shown on the axis labels of the graphs representing histological data.

Cell culture. Rat insulinoma cell line 832/13 (INS-1 β-cells), provided by Christopher B. Newgard (Duke University School of Medicine) (7), were grown in RPMI 1640 supplemented with 11 mM glucose, 10 mM Hepes, 2 mM L-glutamine, 1 mM sodium pyruvate, 100 U/ml penicillin, 100 U/ml streptomycin (Invitrogen), 10% heat-inactivated FBS (Corning) and 50 μM β-mercaptoethanol (Sigma-Aldrich). Murine vascular SMCs were obtained from the aortas of 10-week-old male C57BL/6 mice (Jackson Laboratories) or *Ager*(-/-) mice, as previously described (8) in accordance with institutional guidelines, and were cultured in low glucose DMEM (Invitrogen) supplemented with 10% FBS, 100 U/ml penicillin, and 100 U/ml streptomycin. Cultures were composed of 95% SM-α-actin positivity based on immunostaining. All cultured cells were incubated at 37°C in a humidified 5% CO_2 incubator (9).

Islet isolation and culture. Pancreatic islets were isolated from anesthetized 12-18 week-old male or female C57BL/6 mice (Jackson Laboratories) or *Ager*(-/-) mice (8) according to institutional guidelines. The bile duct was clamped near the sphincter of Oddi, and the pancreas was perfused by ductal injection of ice-cold collagenase solution (2 mg/mL) prepared in HBSS supplemented with 25 mM HEPES (Invitrogen). Pancreas was removed and transferred into HBSS/HEPES solution, digested with oscillation at 37°C, and filtered through a 70 μm filter. Islets were hand purified under a stereo microscope and maintained in RPMI 1640 supplemented with 11 mM glucose, 10 mM Hepes, 2 mM L-glutamine, 1 mM sodium pyruvate, 100 U/ml penicillin, 100 U/ml streptomycin (Invitrogen) and 10% heat-inactivated fetal bovine serum (FBS) (Corning) at 37°C in a humidified 5% CO_2 incubator. For viability and WB studies, islets of consistent size and number were cultured in 96-well (25 islets/well) and 12-well (155 islets/well) plates, respectively, and incubated overnight. Prior to the start of each experiment, cultured islets were assessed by light microscopy to insure that they had viable morphology with intact peripheral mantles.

sRAGE preparation. Human sRAGE was prepared via a baculovirus expression system using Sf9 cells (Clontech; Invitrogen) as previously described (10). sRAGE was purified from serum-free medium via FPLC using HiTrap SP HP purification columns (GE Healthcare). Samples were analyzed by MALDI-TOF Mass Spectrometry (Brucker) or by Electrospray Mass Spectrometry using a Micromass Platform LCZ single quadrupole instrument, to confirm protein identity. The identity of purified human sRAGE was also confirmed by Western blots. Protein amounts were quantified by BCA assay (Pierce).

Thioflavin-T binding assays. In experiments monitoring the kinetics of amyloid formation, the uncertainty in the time measurements on the X-axis is <2 min, which is the length of time that it takes for our fluorimeter to take a read out for each data point. We thus included Y-axis error bars, but not X-axis error bars in order to provide maximal experimental information and prevent clutter in the graphs. To ensure that h-IAPP kinetics data were highly reproducible in h-IAPP/sRAGE binding studies (Figure 3), we used the same primary h-IAPP stock solution in each set of time-course experiments, allowing us to confidently assess our variable of interest: the effect of sRAGE on h-IAPP amyloid formation when sRAGE is added to different h-IAPP kinetic species. Since sRAGE does not interact with fibrillary h-IAPP species, much of it remains suspended in solution causing turbidity, when added to h-IAPP during the growth or saturation phases. The thioflavin-T curves in Figure 3A have thus been normalized to remove artifacts from light scatter using standard methods for comparison of T50 between curves (11). The data presented in Figures 1A and 2C

(carried out at 25°C), and Figure 3A (carried out at 15°C) represent numerous time course experiments, which have been repeated at different times using multiple different preparations of primary peptide stock solutions. The results are highly reproducible under our conditions.

Supplemental References

1. Koch M, Chitayat S, Dattilo BM, Schiefner A, Diez J, Chazin WJ, and Fritz G. Structural basis for ligand recognition and activation of RAGE. *Structure.* 2010;18(10):1342-52.
2. Park H, Adsit FG, and Boyington JC. The 1.5 Å crystal structure of human receptor for advanced glycation endproducts (RAGE) ectodomains reveals unique features determining ligand binding. *J Biol Chem.* 2010;285(52):40762-70.
3. Sturchler E, Galichet A, Weibel M, Leclerc E, and Heizmann CW. Site-specific blockade of RAGE-Vd prevents amyloid-beta oligomer neurotoxicity. *J Neurosci.* 2008;28(20):5149-58.
4. Couce M, Kane LA, O'Brien TD, Charlesworth J, Soeller W, McNeish J, Kreutter D, Roche P, and Butler PC. Treatment with growth hormone and dexamethasone in mice transgenic for human islet amyloid polypeptide causes islet amyloidosis and beta-cell dysfunction. *Diabetes.* 1996;45(8):1094-101.
5. Matveyenko AV, and Butler PC. Islet amyloid polypeptide (IAPP) transgenic rodents as models for type 2 diabetes. *ILAR J.* 2006;47(3):225-33.
6. Jurgens CA, Toukatly MN, Fligner CL, Udayasankar J, Subramanian SL, Zraika S, Aston-Mourney K, Carr DB, Westermark P, Westermark GT, Kahn SE, and Hull RL. β-cell loss and β-cell apoptosis in human type 2 diabetes are related to islet amyloid deposition. *Am J Pathol.* 2011;178(6):2632-40.
7. Hohmeier HE, Mulder H, Chen G, Henkel-Rieger R, Prentki M, and Newgard CB. Isolation of INS-1-derived cell lines with robust ATP-sensitive K+ channel-dependent and -independent glucose-stimulated insulin secretion. *Diabetes.* 2000;49(3):424-30.
8. Toure F, Fritz G, Li Q, Rai V, Daffu G, Zou YS, Rosario R, Ramasamy R, Alberts AS, Yan SF, and Schmidt AM. Formin mDia1 mediates vascular remodeling via integration of oxidative and signal transduction pathways. *Circ Res.* 2012;110(10):1279-93.
9. Travo P, Barrett G, and Burnstock G. Differences in proliferation of primary cultures of vascular smooth muscle cells taken from male and female rats. *Blood Vessels.* 1980;17(2):110-6.
10. Park L, Raman KG, Lee KJ, Lu Y, Ferran LJ, Jr., Chow WS, Stern D, and Schmidt AM. Suppression of accelerated diabetic atherosclerosis by the soluble receptor for advanced glycation endproducts. *Nat Med.* 1998;4(9):1025-31.
11. Tu LH, Serrano AL, Zanni MT, and Raleigh DP. Mutational analysis of preamyloid intermediates: the role of his-tyr interactions in islet amyloid formation. *Biophys J.* 2014;106(7):1520-7.